

Two distinct sequences of blue straggler stars in the globular cluster M30

F.R. Ferraro¹, G. Beccari², E. Dalessandro¹, B. Lanzoni¹, A. Sills³, R. T. Rood⁴, F. Fusi Pecci⁵, A.I. Karakas⁶, P. Miocchi¹ & S. Bovinelli¹

¹*Department of Astronomy, University of Bologna, Via Ranzani, 1, 40127 Bologna, Italy*

²*ESA, Space Science Department, Keplerlaan 1, 2200 AG Noordwijk, Netherlands*

³*McMaster Univ., Dep. of Physics and Astronomy, 1280 Main Street West, Hamilton, Canada*

⁴*Astronomy Department, University of Virginia, P.O. Box 400325, Charlottesville, VA, 22904*

⁵*INAF, Osservatorio Astronomico di Bologna, via Ranzani 1, 40127 Bologna, Italy*

⁶*Research School of Astronomy and Astrophysics, Mt Stromlo Observatory, Weston Creek ACT 2611, Australia*

Stars in globular clusters are generally believed to have all formed at the same time, early in the Galaxy's history¹. 'Blue stragglers' are stars sufficiently massive² that they should have evolved into white dwarfs long ago. Two possible mechanisms have been proposed for their formation: mass transfer between binary companions³, and stellar mergers induced by direct collisions between two stars⁴. Recently, the binary explanation was claimed to be dominant⁵. Here we report on the discovery of two distinct parallel sequences of blue stragglers in M30. This globular cluster is thought to have undergone 'core collapse', during which both the collision rate and the mass transfer activity in binary systems would have

been enhanced⁶. We suggest that the two observed sequences arise from the cluster core collapse, with the bluer population deriving from direct stellar collisions and the redder one arising from the evolution of close binaries which are probably still experiencing an active phase of mass transfer.

To investigate the blue straggler star (BSS) content in M30, we have used a time-series of 44 high-resolution images obtained with the Hubble Space Telescope (see Supplementary Information). The Colour Magnitude Diagram (CMD) derived by combining these measures has revealed the existence of two well-separated and almost parallel sequences of BSS (hereafter Red-BSS and Blue-BSS; Figure 1). The two sequences are similarly populated, consisting of 21 and 24 stars, respectively.

The detected BSS are substantially more concentrated towards the cluster centre than “normal” cluster stars, either along the sub-giant branch (SGB) or the horizontal branch (HB; Figure 2a). Using a Kolmogorov-Smirnov test, the probability that the BSS and the SGB (or HB) populations are drawn from the same distribution is only $\sim 10^{-3}$ (i.e., they differ at more than 4σ significance level). This result confirms that BSS are more massive² than the bulk of the cluster stars and that mass segregation has been active in this cluster. Even more interesting, when we consider the distribution of the two BSS sub-populations separately, we find that the Red-BSS are more centrally segregated than the Blue-BSS. Indeed, no Red-BSS are observed at $r > 30$ arcsec (corresponding to ~ 1.3 pc; see Supplementary Table 1) from the cluster centre (see Figure 2a). Even though in this case the level of significance (1.5σ) is marginal because of the small number of objects, this evidence hints at a different formation history for BSS belonging to the two sequences. Furthermore, while the radial distribution of BSS in many clusters is found to be bimodal⁷ (with a dominant peak at the centre, a dip at intermediate radii and a rising branch in the outer regions), in the case of M30 there is

no evidence of an increase at large distances from the centre: more than 80% of the entire BSS population is confined within the inner 100 arcsec (~ 4.2 pc), and the radial distribution then stays nearly constant for increasing radii. This suggests that the dynamical friction has already affected a large portion of the cluster, so that almost the entire population of BSS has sunk into the centre⁸. There is further evidence that M30 is a highly evolved cluster from a dynamical point of view. The density profile displays a steep power-law cusp in the central 5-6 arcsec (~ 0.2 pc, see Figure 3), suggesting that M30 already experienced the core collapse (CC; see Supplementary Information)⁹. M30's dynamically evolved state, combined with several suggestions^{4,7,10,11} that cluster dynamics and BSS formation processes could be linked, indicates that the dual BSS sequence is likely connected to the cluster dynamical history. In particular, during the CC phase the central density rapidly increases, thus bringing a concomitant increase of gravitational interactions⁶ able to trigger the formation of new BSS via both direct stellar collisions and enhanced mass transfer activity in dynamically shrunk binary systems. Indeed, when considering the entire population of detected BSS ($N_{BSS}=45$) and HB stars ($N_{HB}=90$), the BSS specific frequency ($F^{BSS}=N_{BSS}/N_{HB}$) is equal to 0.5, a value not particularly high compared to other clusters¹². However, the value of F^{BSS} varies significantly over the surveyed area, reaching the value of ~ 1.55 when only the central cusp of the star density profile (5-6 arcsec) is considered (see Figure 2b). This is the highest value ever measured for the BSS specific frequency in any globular cluster, and it further supports the possibility that in M30 we are observing the effect of an enhanced gravitational interaction activity on single and binary stars.

In order to investigate this possibility, we have compared the observations with the predictions of evolutionary models of BSS formed by direct collisions between two Main Sequence stars¹³, with metallicity $Z = 10^{-4}$ and masses ranging between 0.4 and 0.8 M_{\odot} (thus producing BSS with masses between 0.8 and 1.6 M_{\odot}). As shown in Figure 4, the Blue-BSS sequence is well fit by collisional isochrones with ages of 1-2 Gyr, with

the brightest Blue-BSS being slightly less luminous than the collision product of two turnoff-mass stars ($0.8+0.8 M_{\odot}$). Interestingly, the observed number of BSS along the Blue sequence is in good agreement with the expected¹⁴ number of BSS formed by direct collisions during the last 1-2 Gyr in a cluster with total absolute magnitude comparable to that of M30 (see Supplementary Table 1). Hence we conjecture that 1-2 Gyr ago some dynamical process (possibly the CC) produced the BSS population that is now observable along the Blue sequence. In contrast, the origin of the Red-BSS should be different, since this sequence is too red to be properly reproduced by collisional isochrones of any age. Figure 4 also shows the location in the CMD of Single-Star Isochrones (SSIs)¹⁵ computed for a metallicity $Z = 2 \times 10^{-4}$ and shifted by the distance modulus and reddening of M30¹⁶. The 13 Gyr SSI fits the main cluster evolutionary sequences quite well, while the BSS sequences are significantly offset with respect to the 0.5 Gyr SSI, which can be adopted as the cluster zero-age main sequence (ZAMS). Of particular interest is the fact that the Red-BSS sequence is ~ 0.75 mag brighter than the reference ZAMS. Following the results of recent binary evolution models¹⁷, during the mass-transfer phase (which can last several Gyr, i.e., a significant fraction of the binary evolution time-scale), a population of binary systems defines a “low-luminosity boundary” ~ 0.75 mag above the ZAMS in the BSS region (see Figure 5 of Ref. 17). Hence, the BSS that we observe along the Red-sequence could be binary systems still experiencing an active phase of mass-exchange.

Due to the normal stellar evolution, in a few Gyr both collisional and mass-transfer products will populate the region between the two sequences. The fact that we currently see two well-separated sequences supports the hypothesis that both the Blue and the Red-BSS sequences have been generated by a recent and short-lived event, instead of a continuous formation process. A picture where the two BSS sequences are generated by the same dynamical event is therefore emerging. As suggested by the shape of the density profile and by the location of the Blue-BSS in the CMD, 1-2 Gyr ago M30 may

have experienced the CC event. This is known to significantly increase the gravitational interaction rate and therefore it may have boosted the formation of BSS: the Blue-BSS arise from direct stellar collisions, while the Red-BSS are the result of the evolution of binary systems which first sank into the cluster centre because of the dynamical friction (or they were already present into the cluster core), and then have been brought into the mass-transfer regime by hardening processes induced by gravitational interactions during the CC phase. Indeed, the detected double BSS sequence could be the signature of the CC phenomenon imprinted onto a stellar population, with the Red-BSS sequence being the outcome of the “binary-burning” process expected to occur in the cluster core during the late stages of the CC^{18,19}. The proposed picture leads to a testable observational prediction: the Red-BSS sequence should be populated by binaries with short orbital periods.

A recent paper⁵ suggested that the dominant BSS formation channel is the evolution of binary systems, independently of the dynamical state of the parent cluster. Our discovery shows that binary evolution alone does not paint a complete picture: dynamical processes can indeed play a major role in the formation of BSS. An appropriate survey of the central regions of other post-core collapsed clusters is urged in order to clarify whether the double BSS sequence is a common signature of the CC phenomenon. Moreover, detailed spectroscopic investigations are certainly worth performing to obtain a complete characterization of the BSS properties (orbital periods, rotation velocities, etc.). In this respect particularly promising is the search for the chemical signature²⁰ of the mass-transfer process for the BSS along the red sequence, even if, in the case of M30, this will push the performances of the current generation of high-resolution spectrographs mounted at 8-m class telescopes to their limit.

1. Marín-Franch, A. *et al.* The ACS Survey of Galactic Globular Clusters. VII. Relative Ages. *Astrophys. J.* **694**, 1498-1516 (2009)
2. Shara, M. M., Saffer, R. A., & Livio, M. The First Direct Measurement of the Mass of a Blue Straggler in the Core of a Globular Cluster: BSS19 in 47 Tucanae *Astrophys. J. Lett.* **489**, L59-L63 (1997)
3. McCrea, W. H. Extended main-sequence of some stellar clusters. *Mon. Not. R. Astron. Soc.* **128**, 147-155 (1964)
4. Hills J. G., & Day, C. A. Stellar Collisions in Globular Clusters. *Astrophys. J. Lett.* **17**, 87 (1976)
5. Knigge, C., Leigh, N. & Sills, A. A binary origin for 'blue stragglers' in globular clusters, *Nature*, **457**, 288-290 (2009)
6. Meylan, G. & Heggie, D.C., Internal dynamics of globular clusters. *Ann. Rev. Astron. & Astrophys.* **8**, 1-143 (1997)
7. Ferraro, F.R. & Lanzoni, B. Blue Straggler Stars in Galactic Globular Clusters: Tracing the Effect of Dynamics on Stellar Evolution. In *Dynamical Evolution of Dense Stellar Systems*, Proceedings of the International Astronomical Union, IAU Symposium, **246**, 281-290 (2008)
8. Mapelli, M., Sigurdsson, S., Ferraro, F. R., Colpi, M., Possenti, A. & Lanzoni, B. The radial distribution of blue straggler stars and the nature of their progenitors. *Mon. Not. R. Astron. Soc.* **373**, 361-368 (2006)
9. Trager, S. C., Djorgovski, S. & King, I.R., Structural parameters of Galactic Globular Clusters in *Structure and Dynamics of Globular Clusters*, Editors, S.G. Djorgovski and G. Meylan; Publisher, *Astronomical Society of the Pacific Conference Series*, **Vol. 50**, 347-355 (1993)

10. Baily, C. D. Are there two kinds of blue stragglers in globular clusters? *Astrophys. J.* **392**, 519-521 (1992)
11. Leonard, P.J.T. Stellar collisions in globular clusters and the blue straggler problem. *Astronom. J.*, **98**, 217-226 (1989)
12. Ferraro, F. R., Sills, A., Rood, R.T., Paltrinieri, B. & Buonanno, R. Blue Straggler Stars: A Direct Comparison of Star Counts and Population Ratios in Six Galactic Globular Clusters. *Astrophys. J.* **588**, 464-477 (2003)
13. Sills, A., Karakas, A.I. & Lattanzio, J. Blue Stragglers After the Main Sequence. *Astrophys. J.* **692**, 1411-1420 (2009)
14. Davies, M.B., Piotto, G. & de Angeli, F., Blue straggler production in globular clusters *Mon. Not. R. Astron. Soc.* **349**, 129-134 (2004)
15. Cariulo, P., Degl'Innocenti, S. & Castellani, V. Calibrated stellar models for metal-poor populations. *Astron. & Astrophys.* **421**, 1121-1130 (2004)
16. Ferraro, F.R., Messineo, M., Fusi Pecci, F., De Palo, M.A., Straniero, O., Chieffi, A. & Limongi, M. The Giant, Horizontal, and Asymptotic Branches of Galactic Globular Clusters. I. The Catalog, Photometric Observables, and Features. *Astronom. J.*, **118**, 1738-1758 (1999)
17. Tian, B., Deng, L. , Han, Z. & Zhang, X.B. The blue stragglers formed via mass transfer in old open clusters. *Astron. & Astrophys.* **455**, 247-254 (2006)
18. McMillian, S., Hut, P. & Makino, J. Star cluster evolution with primordial binaries. I - A comparative study. *Astrophys. J.* **362**, 522-537 (1990)
19. Hurley, J., et al. Deep Advanced Camera for Surveys Imaging in the Globular Cluster NGC 6397: Dynamical Models. *Astronom. J.*, **135**, 2129-2140 (2008)

20. Ferraro, F.R., et al. Discovery of Carbon/Oxygen-depleted Blue Straggler Stars in 47 Tucanae: The Chemical Signature of a Mass Transfer Formation Process. *Astrophys. J. Lett.* **647**, L53-L56 (2006)
21. Stetson, P.B. DAOPHOT - A computer program for crowded-field stellar photometry. *PASP*, **99**, 191-222 (1987)
22. Stetson, P.B. The centre of the core-cusp globular cluster M15: CFHT and HST Observations, ALLFRAME reductions. *PASP*, **106**, 250-280 (1994)
23. Pietrukowicz, P., & Kaluzny, J. Variable Stars in the Archival HST Data of Globular Clusters M13, M30 and NGC 6712. *Acta Astronomica*, **54**, 19-31 (2004)
24. Vilhu, O. Detached to contact scenario for the origin of W UMa stars. *A&A*, **109**, 17-22 (1982)
25. Hartigan P., Applied Statistics, Vol. 34, N. 3, p. 320 (1985)
26. King, I.R. The structure of star clusters. III. Some simple dynamical models. *Astronom. J.* **71**, 64-75 (1966)
27. Harris, W.E. A Catalog of Parameters for Globular Clusters in the Milky Way. *Astronom. J.*, **112**, 1487-1488 (1996)
28. Noyola, E. & Gebhart, K. Surface Brightness Profiles for a Sample of LMC, SMC, and Fornax Galaxy Globular Cluster. *Astronom. J.*, **132**, 447-466 (2006)
29. Djorgovski, S. Physical parameters of Galactic Globular Clusters in *Structure and Dynamics of Globular Clusters*, Editors, S.G. Djorgovski and G. Meylan; Publisher, *Astronomical Society of the Pacific Conference Series*, **Vol. 50**, 373-382 (1993)

Acknowledgements: This research was supported by “Progetti di Ricerca di Interesse Nazionale 2008” granted by the Istituto Nazionale di Astrofisica. We acknowledge the financial support of the Agenzia Spaziale Italiana and the Ministero dell'Istruzione, dell'Università e della Ricerca. FRF, BL, ED and AS thank the “Formation and evolution of Globular Clusters programme” and the Kavli Institute for Theoretical Physics in Santa Barbara (California, USA) for the hospitality during their stay, when the motivations of this project were discussed and the work planned. We acknowledge support from the ESTEC Faculty Visiting Scientist Programme. RTR is partially supported by a STScI grant. This research has made use of the ESO/ST-ECF Science Archive facility which is a joint collaboration of the European Southern Observatory and the Space Telescope - European Coordinating Facility.

Author contributions: F.R.F. designed the study and coordinated the activity. G.B., E.D. and S.B. analysed the data. A.S. and A.I.K. developed collisional models. B.L. and P.M. computed the surface density profile and performed comparisons with a single mass King model. F.R.F. and B.L. wrote the paper. F.F.P., A.S. and R.T.R. critically contributed to the paper discussion and presentation. All the authors contributed to discuss the results and commented on the manuscript.

Correspondence to: F.R.Ferraro¹ Correspondence and requests for materials should be addressed to F.R.F.

francesco.ferraro3@unibo.it

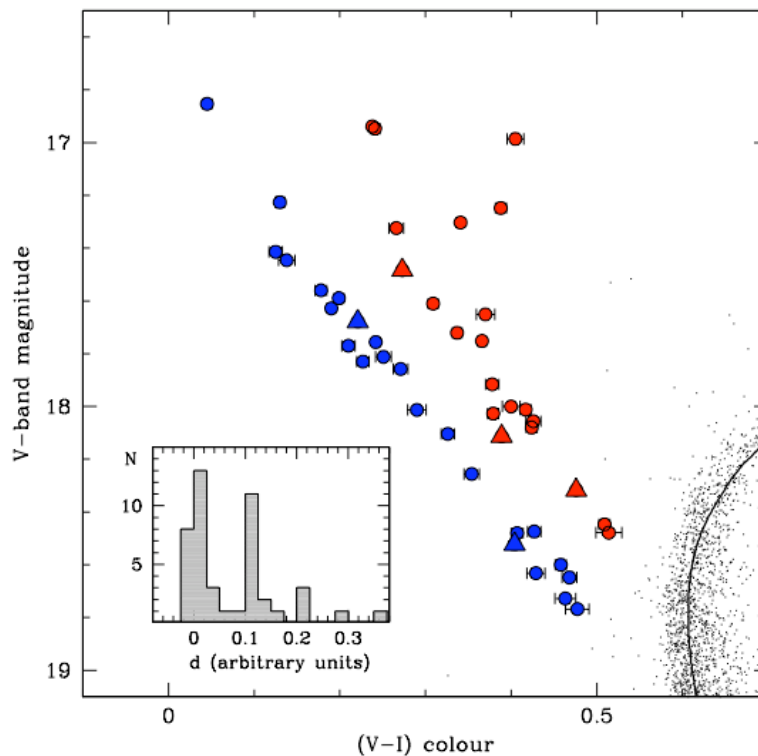


Figure 1. The two blue straggler sequences of M30. ($V, V-I$) CMD zoomed in the BSS region. The selected BSS are plotted as large circles, with the red and blue colours distinguishing the Red- and the Blue-BSS sequences, respectively. A series of 44 images (22 in each filter), secured with the Wide Field Planetary Camera 2 (WFPC2) through the F814W (I) and the F555W (V) filters, has been analyzed by using PSF-fitting photometry^{21,22}. Errors (1 s.e.m) in magnitude and colours have been computed from repeated measures and are also plotted (they are typically lower than 0.01 mag; in most cases the error bars are smaller than the circle size). The two sequences are separated in magnitude by $\Delta V \sim 0.4$ mag and in colour by $\Delta (V-I) \sim 0.12$ mag.

By exploiting the secured time-series, we have tested the variability of the selected BSS and found 5 candidate variables (triangles): based on the light curve characteristics, the three brightest variables have been classified²³ as W Uma contact binaries, while the two faintest candidates show quite scattered

light curves which prevent a reliable classification. W Uma stars are binary systems losing orbital momentum because of magnetic braking. These shrinking binary systems, initially detached, evolve to the contact stage and finally merge into a single star. The evolution of W UMa systems is thought to be a viable channel for the formation of BSS^{20,24}. The inset shows the distribution of the geometrical distances (in arbitrary units) of the selected BSS from the straight line that best-fits the Blue-BSS sequence. Two well defined peaks are clearly visible. A *Dip-test*²⁵ applied to this distribution demonstrates that it is bimodal at more than 4σ significance level, thus confirming that the two sequences are nearly parallel to each other.

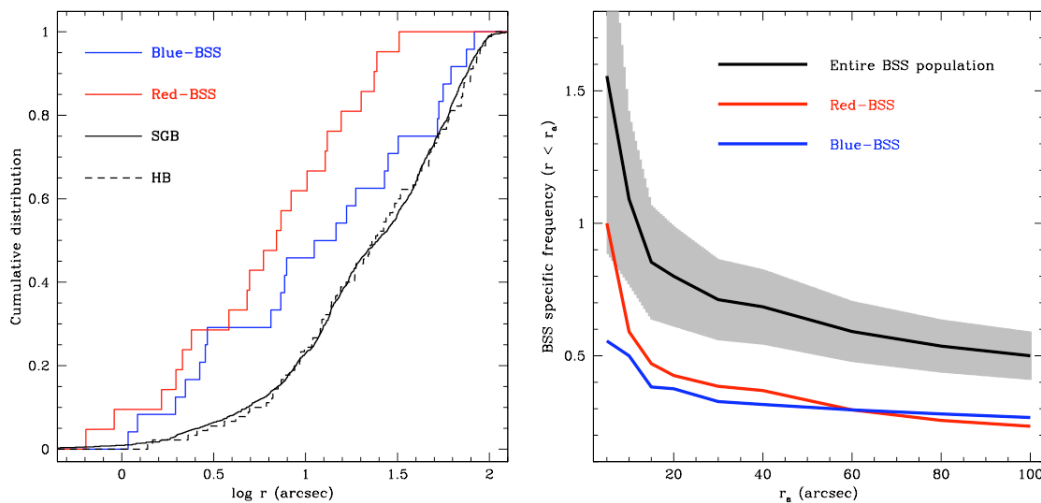


Figure 2. The BSS radial distribution.

a, Cumulative radial distribution of Red-BSS (red line) and Blue-BSS (blue line), as a function of the projected distance from the cluster centre of gravity. The distribution of SGB stars (solid black line) and HB stars (dashed black line) is also plotted for comparison.

b, BSS specific frequency (i.e., the ratio between the number of BSS and that of HB stars) computed in circular areas of increasing radius r_a . The lines refer to the overall BSS population (in black), and to the Red-BSS and Blue-BSS sub-populations separately (in red and blue, respectively). The grey area around the black line shows the 1σ s.d. uncertainty in the specific frequency. As apparent, BSS are substantially more numerous than HB stars in the cluster centre. Although the small number of stars in the sample prevents statistically robust results, we note that in the innermost 5-6 arcsec (~ 0.2 pc) the Red-BSS tend to be as numerous as the HB stars and dominate the ratio.

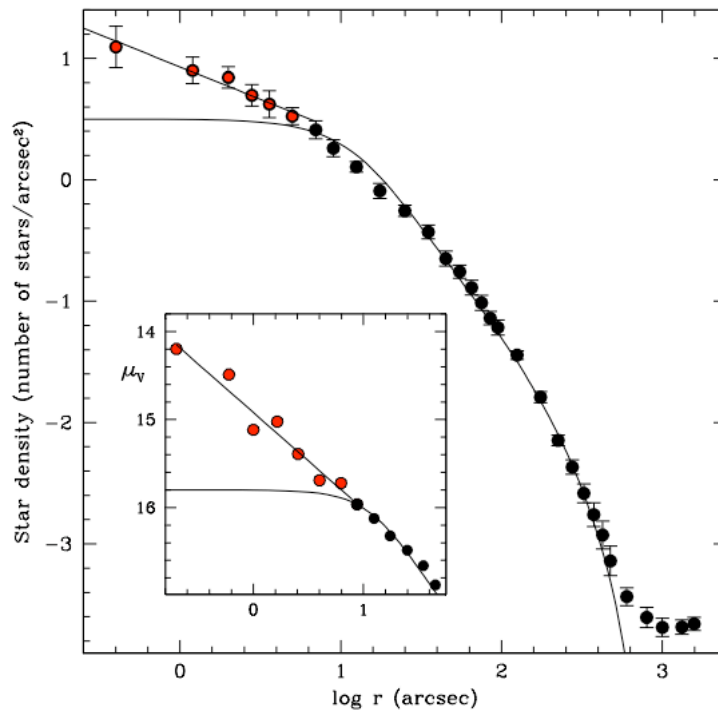


Figure 3. The star density profile of M30. The profile (plotted error bars are 1 s.e.m) has been obtained by resolved star counts over the entire cluster extension: the WFPC2 dataset has been combined with ACS data and with wide field ground-based observations secured at the ESO-NTT and CHFT-MEGACAM. The single-mass King model²⁶ that best fits the observed profile excluding the innermost ($r < 5$ arcsec) points is shown as a thick solid line. The points that deviate from the King profile (shown as red dots) are well fit by a power-law with slope $\alpha \approx -0.5$ (thin solid line). The inset displays the surface brightness profile derived from the WFPC2-V images within the innermost 40 arcsec, with the two lines having the same meaning as above. The measured central surface brightness is $\mu_V \sim 14.2$ mag arcsec⁻². This value is significantly brighter than that listed in currently adopted cluster catalogs²⁷, but fully consistent with that obtained in most recent studies²⁸. Following the procedure described in the literature²⁹ and adopting a distance of 8.75 kpc and a reddening $E(B-V) = 0.03$ ¹⁶, we derived $\nu \sim 9.6 \times 10^4 L_\odot \text{pc}^{-3}$ for the luminosity

density within the density cusp (i.e., for $r < 5$ arcsec). Under the assumption of a mass-to-light ratio $M/L = 3$ and a mean stellar mass $\langle m \rangle = 0.5 M_{\odot}$, this corresponds to a number density of stars $n \sim 5.8 \times 10^5 \text{ pc}^{-3}$ (see Supplementary Table 1).

Both the profiles have been computed with respect to the newly determined cluster centre of gravity (see Supplementary Table 1). This new determination is located at $\sim 3''$ South-East with respect to the centre listed in commonly adopted globular cluster catalogs²⁷.

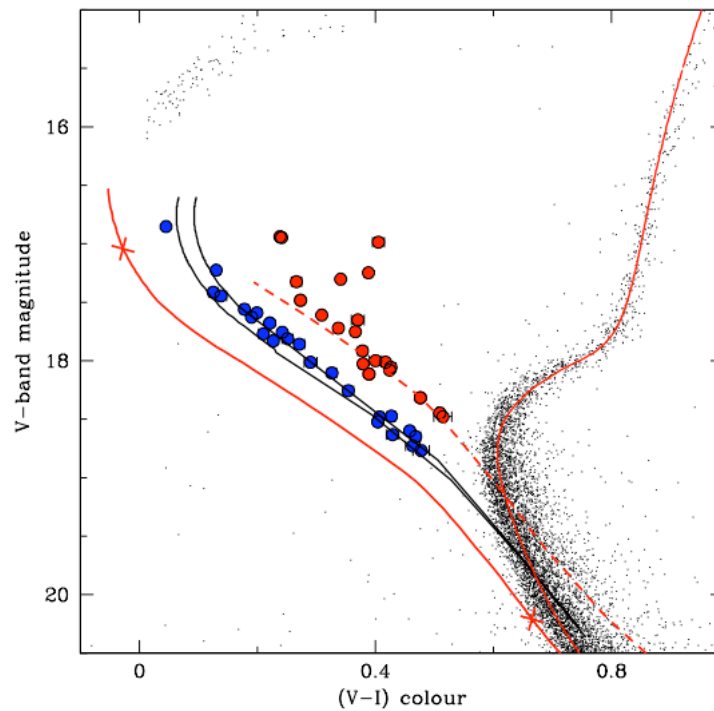


Figure 4. Comparison with collisional and binary evolution models. An enlarged portion of the CMD of M30 is shown. The solid black lines correspond to the collisional isochrones¹³ at 1 and 2 Gyr, that nicely reproduce the Blue-BSS sequence. The red solid lines correspond to the Single-Star Isochrones¹⁵ at 13 Gyr (well fitting the main cluster evolutionary sequences) and at 0.5 Gyr (representing the reference cluster ZAMS). The two crosses mark the position of a 0.8 and a 1.6 M_{\odot} star along the ZAMS. The red dashed line corresponds to the ZAMS shifted by 0.75 mag, thus marking the position of the ‘low-luminosity boundary’ predicted¹⁷ for a population of mass-transfer binary systems. As apparent, this line well reproduces the Red-BSS sequence.

Supplementary Information

Data-set: The data-set used in this study consists of a series of 44 images (22 in filter F814W and 22 in filter F555W) secured in 1999 with the Wide Field Planetary Camera 2 (WFPC2) on board the Hubble Space Telescope. Exposures have been obtained within a project (GO-7379, PI: Edmonds) aimed at searching for stellar variability, from main sequence binaries, cataclysmic variables and blue stragglers, in the congested core of M30^{23,30}.

Core collapse: The core collapse is a catastrophic dynamical process consisting in the runaway contraction of the core of a star cluster⁶. Binary-binary and binary-single collisions are thought to halt (or delay) the collapse of the core, thus avoiding infinite central densities⁶. A common core-collapse observational signature is a steep cusp in the projected star density profile. About 15% of the globular cluster population in our Galaxy (including M30) shows evidence of this phenomenon⁹.

Supplementary Table 1

Table 1 Cluster parameters

Centre of gravity	$\alpha=21^{\text{h}}40^{\text{m}}22.13^{\text{s}}$ $\delta=-23^{\circ}10'47.4''$
Central surface brightness	$\mu_V = 14.2 \text{ mag arcsec}^{-2}$
Physical size of the central cusp	$r_{\text{cusp}} = 0.2 \text{ pc}$
Central mass density [$M_{\odot} \text{ pc}^{-3}$]	$\text{Log } \rho_0 = 5.48$
True distance modulus ¹⁶	$(m-M)_0 = 14.71 \text{ mag}$
Colour excess ¹⁶	$E(B-V) = 0.03 \text{ mag}$
Distance ¹⁶	$d = 8.75 \text{ kpc}$
Integrated V magnitude ²⁷	$V=7.19 \text{ mag}$
Integrated absolute magnitude	$M_V = -7.61 \text{ mag}$
Age	$t = 13 \text{ Gyr}$
Metallicity ¹⁶	$[\text{Fe}/\text{H}] = -1.9$

Supplementary References

30. Lugger, P. M.; Cohn, H. N., Heinke, C. O., Grindlay, J. E. & Edmonds, P.D.
 Variable Chandra X-Ray Sources in the Collapsed-Core Globular Cluster M30
 (NGC 7099). *Astrophys. J.* **657**, 286-301 (2007)